

Multilevel inverter application for railway traction motor control

Vo Thanh Ha¹, Pham Thi Giang², Phuong Vu³

¹Faculty of Electrical and Electrical Engineering, University of Transport and Communications, Hanoi, Vietnam

²Faculty of Electrical Engineering, University of Economics-Technology for Industries, Hanoi, Vietnam

³School of Electrical and Electronics Engineering, Hanoi University of Science and Technology, Hanoi, Vietnam

Article Info

Article history:

Received Apr 16, 2022

Revised May 15, 2022

Accepted Jun 15, 2022

Keywords:

CHB

FC

H-Bridge cascaded

Multilevel inverter

NPC

Railway traction motor

ABSTRACT

This paper will present why choosing a 7-level reverse voltage source fed to three-phase induction motors to the railway traction motor. In addition, this paper shows the implementation of space vector pulse width modulation (SVPWM) and the math model of induction motor, stator currents, and speed controller design of electric traction drive system based on field-oriented control (FOC). By MATLAB/Simulink method, this multi-level inverter in FOC structure reduces total harmonic distortion (THD) more than other multi-level inverters such as 3 and 5-level inverter. Furthermore, this FOC control structure combined with 7-level inverter improved speed and torque responses required for railway traction motor load.

This is an open access article under the [CC BY-SA](https://creativecommons.org/licenses/by-sa/4.0/) license.



Corresponding Author:

Phuong Vu

School of Electrical and Electronics Engineering, Hanoi University of Science and Technology
Hanoi, Vietnam

Email: phuong.vuhoang@hust.edu.vn

1. INTRODUCTION

Since the 1990s, the 3-phase AC induction motors (IMs) have been widely used for the railway traction motor (RTM), which has replaced DC motors. The main reason for replacing DC motor is because the IMs have more advantages of low cost, high mechanical durability, and in addition, they can be operated at weakling flux and applied linear, nonlinear methods to torque and speed control with good and requirement responses suitable for RTW [1]-[4]. Additionally, electrical RTM has been being studied by scientists in theory and also experimentation. Because this electrical transport system is prevalent in developed and developing countries. The transport system aims to reduce traffic congestion in the big city [5]-[7]. The electric railway system with a large capacity (200 kW-300 kW) and requires a transformer from high voltage (25 kV, 50 Hz) to low voltage (1500 V-750 V, 50 Hz), which is fed to the RTM [8], [9]. Moreover, the RTW commands high voltage operation, so it needs a power inverter to ensure total harmonic distortion (THD) of stator currents and torque rippor as required to create the speed and torque responses with characteristics suitable for RTM.

In the control structure, the control structure mainly used the 2-level inverter, a simple system, and easy pule comprehensive modules such as PWM, SVM. However, it has a THD higher than a multilevel converter [10], [11]. According to Van *et al.* [10], the multilevel inverter is constructed by power semiconductor devices and a DC voltage source, their output generating voltage with step waveform. By increasing the number of level voltage in the multilevel inverter, the output voltage forms a sine wave with reduced THD. The multilevel inverter has had common three types of neutral point clamped (NPC), flying capacitor (FC), and cascaded H-bridge (CHB) are applied in industry, civil, transport such as pumps, fans, wind

energy, and railway traction motor. The NPC multilevel inverter with advantage reduced TDH than more THD of 2-level invert. However, it is difficult to expand the step of voltage levels because this inverter structure should increase the number of diodes switchgear, making the system unrealized. In addition, the capacitor-clamped multilevel inverter has had a structure like a diode-clamped multilevel inverter [12]-[14].

However, in this structure, FC the leg diodes have been replaced by a leg capacitor. FC has connected by a capacitor following the ladder, where the voltage on each capacitor differs. Therefore, it will vary with the following voltage capacitors. Thus, the FC has the advantage that it does not require all consecutive semiconductors as NPC. Moreover, the THD is lower than the TDH of NPC. Although the voltage step can be creased as necessary, the more significant number of capacitors is more expensive than NPC [15]-[19]. Then, the H-bridge multilevel inverter (CHB) has an m-level cascaded converter structure [20], [21]. This CHB multilevel inverter uses an IGBT semiconductor and a separate DC source (multi-output by transformer or capacitors). This multilevel inverter is an advantage more than NPC and FC, such as the voltage level with inverter cascaded is designed and installed easily, and the THD is reduced as required. In addition, This CHB inverter is comfortable for medium-high voltage. Moreover, this structure needs DC balancing; thus, control must be designed for the voltage balance algorithm in the system. Thereby the advantages and disadvantages of the three multilevel above analyses, so the CHB multilevel inverter will suit a railway traction motor with a high voltage requirement. Furthermore, inverters can be stacked at practically unlimited levels [22]-[25]. In addition, the paper presented the control structure of the traction drive system using CHB multilevel converter based on the FOC control method with the currents; the speed controller is designed to have good responses to demonstrate the advantage of a multilevel CHB multilevel converter that can reduce THD.

The paper is presented the 7-level CHB multilevel inverter application for railway traction motor based on the FOC control method. The paper consists of sections following section 2 will show the pulse width modulated voltage of a 7-level CHB multilevel inverter by the SVM method. Then, section 3 gives the math model of the three-phase induction motor and load model. Next, some results demonstrate MATLAB/Simulink shows the effectiveness of the proposed solution. Finally, some evaluate the conclusion of the 7-level CHB multilevel inverter, speed, and the torque responses are presented in the section conclusion.

2. THE SPACE VECTOR WIDTH MODULATION OF THE 7-LEVELS INVERTER FOR CHB STRUCTURE

2.1. The 7-level voltage inverter control structure

The three-phase structure of the cascaded H-bridge 7-level converter is shown in Figure 1, which is a coupling for three diagrams of the 1-phase. The output of this converter is the three-phase voltage that is 120° out of phase as shown in the (1).

$$\begin{aligned} u_A &= 3E \sin(\omega t) \\ u_B &= 3E \sin(\omega t - 2\pi/3) \\ u_C &= 3E \sin(\omega t + 2\pi/3) \end{aligned} \quad (1)$$

The form of a 3-phase reverse flow output voltage connected to the H-bridge cascade is shown in Figure 2. To generate voltage 7 levels, there must be coordination switching valves in each phase at each H-bridge. In each bridge diagram and at any given moment, there are only two open-ended semiconductor valves; the other two valves are locked. The control for 3-phase voltage generation is just three sine waves controlled 120° difference at 3 phases. At $S_{11}, S_{21}, S_{12}, S_{22}, S_{13}, S_{23}$ are opened thus, this leads to the following results as $U_{AN} = U_{h1} + U_{h2} + U_{h3} = 3E$. With such an argument, analysis than at $S_{31}, S_{41}, S_{32}, S_{42}, S_{33}, S_{43}$ are opened thus $U_{AN} = -3E$. From the structure of the inverter in Figure 1 and the simulation in Figure 2, there are the following comments:

- The required load voltage is high, but the reverse output voltage per H-bridge is small, which limits the valves being subjected to too high voltages, furthermore still meeting the needs of the load.
- The inverted output voltage has the form of the multi-step ladder as a sine wave than fundamental inversion.
- The switching frequency is minor, usually below 1kHz.
- Low distortion output current is the most significant advantage of this scheme.
- A large number of independent DC sources must be used.
- A large number of switching valves for the system leads to a complicated control of switching valves with increasing levels. This three-phase structure of the 7-level converter with 3 H-bridge inverters requires 36 semiconductor valves for switching. The H-bridge in the same phase follows a standard sine wave. The carrier by number of H-bridge, including the M carriers. These carriers have the same frequency and the same peak amplitude. However, there is a phase shift between two adjacent pages at an angle.

$$\varphi_{cr} = 360^\circ / (N - 1) \quad (2)$$

The coefficient of frequency modulation and amplitude modulation are written in (3)

$$m_f = \frac{f_{car}}{f_{ref}}; m_a = \frac{A_{ref}}{A_{car}} \quad (3)$$

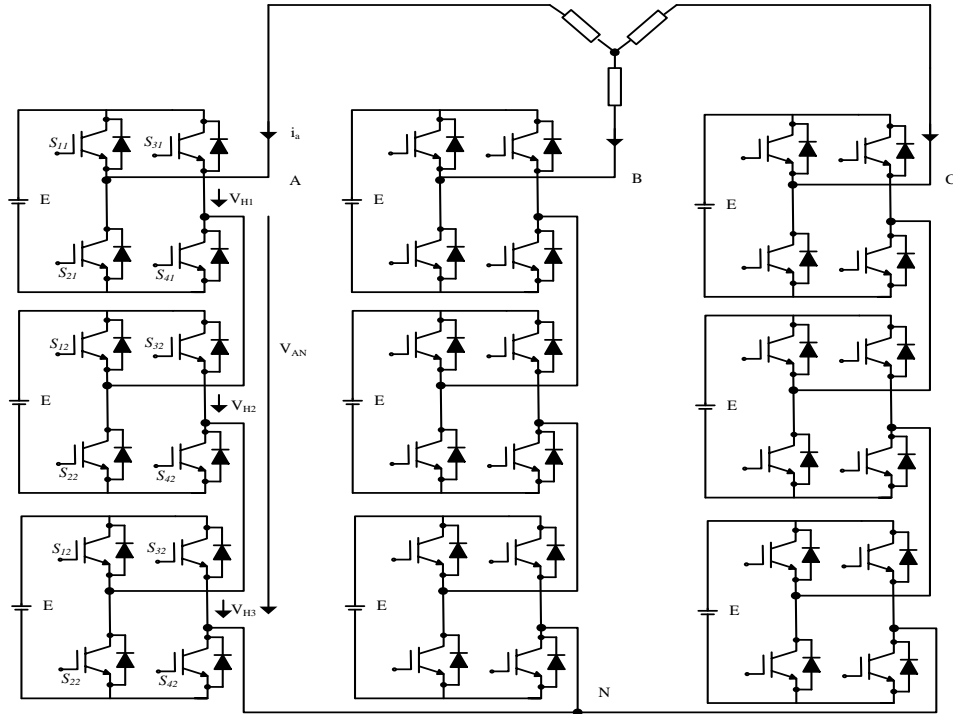


Figure 1. Three-phase structure of the cascaded H-bridge 7-level converter

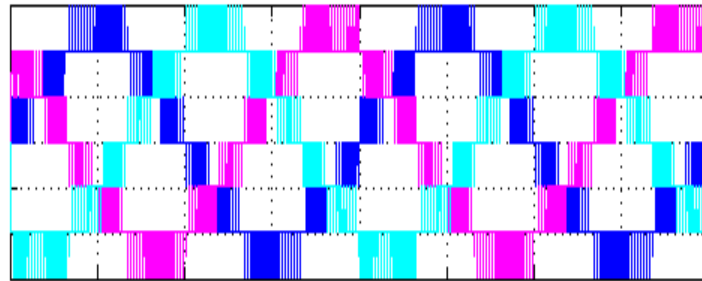


Figure 2. The formatted output voltage inverter for 3 phase voltages with cascaded H-bridge 7-level converter

2.2. The SVM for 3 phase voltages with the cascaded H-bridge 7-level converter

With a multi-level inverse scheme, the number of sub-triangles on the vector plane will increase rapidly as the number of levels (M) increases. The calculation will become simpler if using the system's symmetry in every corner vector space sixth. It was shown on three vector plane coordinate system quadrant six (Z_{1x}, Z_{1y}) , (Z_{2x}, Z_{2y}) , (Z_{3x}, Z_{3y}) . The number of sub-triangles in the space vector diagram will be much increased as the level increases. The calculation becomes much easier using the symmetry characteristic of the space vectors system in each sector. The coordinate systems (Z_{1x}, Z_{1y}) , (Z_{2x}, Z_{2y}) and (Z_{3x}, Z_{3y}) are shown Figure 3. Firstly, determine the projection of the desired voltage vector on the coordinate system $\mathbf{v}_r = [v_{r\alpha}, v_{r\beta}]^T$ on (Z_{1x}, Z_{1y}) , (Z_{2x}, Z_{2y}) and (Z_{3x}, Z_{3y}) . Then define three transform matrices M_1 , M_2 and M_3 defined as follows in (5).

$$\begin{cases} v_\alpha = v_A \\ v_\beta = \frac{1}{\sqrt{3}}(v_B - v_C) \end{cases} \quad (4)$$

$$M_1 = \begin{bmatrix} 1 & -\frac{1}{\sqrt{3}} \\ 0 & \frac{2}{\sqrt{3}} \end{bmatrix}; M_2 = \begin{bmatrix} 1 & \frac{1}{\sqrt{3}} \\ -1 & \frac{1}{\sqrt{3}} \end{bmatrix}; M_3 = \begin{bmatrix} 0 & \frac{2}{\sqrt{3}} \\ -1 & -\frac{1}{\sqrt{3}} \end{bmatrix} \quad (5)$$

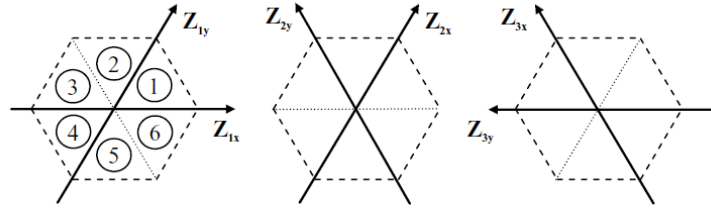


Figure 3. The coordinate systems as (Z_{1x}, Z_{1y}) , (Z_{2x}, Z_{2y}) and (Z_{3x}, Z_{3y})

According to [10] paper, if SVM for the multilevel inverter is to be successful, the following steps are required.

Step 1: Determination of reference vector location

The sector number S ($S=I, II, \dots, VI$) can be determined in Table 1.

Table 1. The sector determination algorithm

$z_{1x}, z_{1y} < 0$				$z_{1x}, z_{1y} \geq 0$	
$z_{2x}, z_{2y} < 0$		$z_{2x}, z_{2y} \geq 0$		$z_{1x} < 0$	$z_{1x} \geq 0$
$z_{3x} < 0$	$z_{3x} \geq 0$	$z_{2x} < 0$	$z_{2x} \geq 0$	Sec IV	Sec I
Sec III	Sec VI	Sec V	Sec II		

Step 2: The determination of duty cycles

This is determining the nearest three vectors based on the three vertices of the modulation triangle, calculating the duty cycles of the identified nearest three vectors and determining the switching state of the inverter. For instance, as shown Figure 4.

The vector of \vec{V}_1 can be represented by $\vec{p}_1, \vec{p}_2, \vec{p}_3$ vectors in the (6):

$$\vec{V}_1 = \vec{p}_1 + m_g(\vec{p}_2 - \vec{p}_1) + m_h(\vec{p}_3 - \vec{p}_1) = (1 - m_g - m_h)\vec{p}_1 + m_g\vec{p}_2 + m_h\vec{p}_3 \quad (6)$$

The vector of \vec{V}_1 can be represented by $\vec{p}_2, \vec{p}_3, \vec{p}_4$ vectors in (7).

$$\begin{aligned} \vec{V}_2 &= \vec{p}_4 + (1 - m_g)(\vec{p}_3 - \vec{p}_4) + (1 - m_h)(\vec{p}_2 - \vec{p}_4) \\ &= (m_g + m_h - 1)\vec{p}_4 + (1 - m_g)\vec{p}_3 + (1 - m_h)\vec{p}_2 \end{aligned} \quad (7)$$

Where m_g, m_h are defined by (8).

$$\begin{cases} m_g = z_{1x} - \lfloor |z_{1x}| \rfloor = z_{1x} - k_g \\ m_h = z_{1y} - \lfloor |z_{1y}| \rfloor = z_{1y} - k_h \end{cases} \quad (8)$$

With: $k_g = \lfloor |z_{1x}| \rfloor, k_h = \lfloor |z_{1y}| \rfloor$

Step 3: Determination of the switching states

If the $k_A=k$ coefficient, thus k coefficient must satisfy this condition: $-\frac{M-1}{2} \leq k \leq \frac{M-1}{2}$, the coordinates of state vectors in (a, b, c) coordinates system is given by (9). In (9) shows the relationship between $[k_{ix}, k_{iy}]$ coordinate ($i=1,2,3$) and (a, b, c) coordinate.

$$\begin{bmatrix} k_{1x} \\ k_{1y} \end{bmatrix} \approx \begin{bmatrix} k_{AN} \\ k_{BN} \\ k_{CN} \end{bmatrix} = \begin{bmatrix} k \\ k - k_{1x} \\ k - k_{1x} - k_{1y} \end{bmatrix} \quad (9)$$

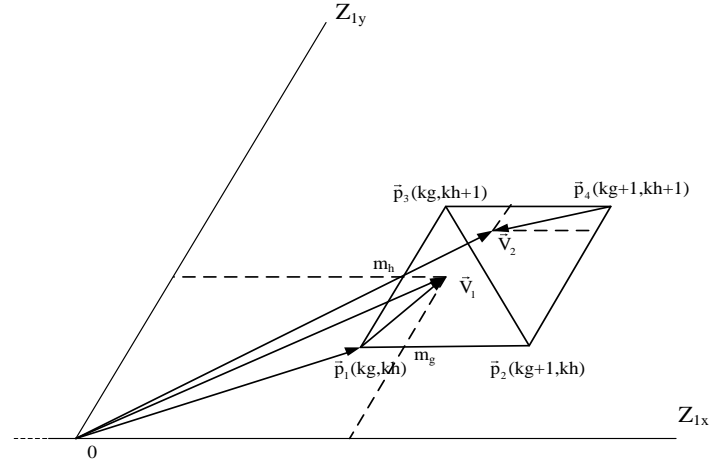


Figure 4. The reference vector can be synthesized by the three nearest vectors

3. THE MODEL OF INDUCTION MOTOR AND LOAD MODEL OF RTM

3.1. The model of induction motor

The FOC control method, for controlling the motor IM like AC motor, because by converting coordinates, found two electric currents to operate the stator flux and torque. Although the dq coordinate is the rotational coordinate, the model's IM appears to be a nonlinear component [4]. Thus, the FOC method, IM's mathematical model, is described by (10).

$$\begin{cases} \frac{di_{sd}}{dt} = -\left(\frac{1}{\sigma T_s} + \frac{1-\sigma}{\sigma T_r}\right)i_{sd} + \omega_s i_{sq} + \frac{1-\sigma}{\sigma T_r} + \frac{1}{\sigma L_s}u_{sd} \\ \frac{di_{sq}}{dt} = -\omega_s i_{sd} - \left(\frac{1}{\sigma T_s} + \frac{1-\sigma}{\sigma T_r}\right)i_{sq} - \frac{1-\sigma}{\sigma} \omega i_m + \frac{1}{\sigma L_s}u_{sq} \\ \frac{d\psi_{rd}}{dt} = -\frac{1}{T_r}\psi_{rd} + \frac{L_m}{T_r}i_{sd} \\ \frac{d\omega}{dt} = k_\omega \psi_{rd} i_{sq} - \frac{z_p}{J}m_L \end{cases} \quad (10)$$

With $\omega_s = \omega + \omega_r = \omega + \frac{L_m}{T_r} \frac{i_{sq}}{\psi_{rd}}$; $k_\omega = \frac{3}{2} \frac{z_p^2 L_m^2}{L_r J}$

In which, $i_{sd}; i_{sq}$ are dq components of the stator current; i_m is electromagnetic currents; ω, ω_s are mechanical and synchronous speed, respectively; ψ'_{rd}, ψ'_{rq} are dq components of the rotor flux; σ is total leakage factor; T_r is rotor time constant; u_{sd}, u_{sq} are dq components of the stator voltage; L_s is stator inductance, L_m, L_r are mutual, rotor inductance, m_L : torque load. It can be seen that the original state (10) is bilinear and is of 4th order. The mechanical equation of an IM can be showed by (11).

$$m_M = m_T + \frac{J d\omega}{dt} \quad (11)$$

Where: J is inertia torque constant; ω is the rotor mechanical speed; m_T is load torque. The load torque the sum of the resistance forces against motion of RTM. The load mode is calculated by the following as (12).

$$F(t) = a_{11}M + a_{12}n + a_2 Mv(t) + a_3 A k v(t)^2 + Mg \sin \alpha \quad (12)$$

Where, M, n, A, k, α represent the weight of the train, the shaft, the surface area in the direction of displacement, the track and gear parameters; v is train speed.

4. SIMULATION RESULTS

The structure of 7 level H-bridge cascade inverter with the stator currents and speed control for an IM used in a RTW is presented in Figure 5 and simulation with parameters of 7 level H-bridge cascade inverter and IM's parameters used railway traction motor follow as Table 2. In Figure 5, the stator current controller is PI with $K_p = 0.385$; $T_i = 0.052$ coefficients. The speed controller is PI with $K_p = 4.1$; $T_i = 0.82$ coefficients. This coefficients, current controller response is perfect.

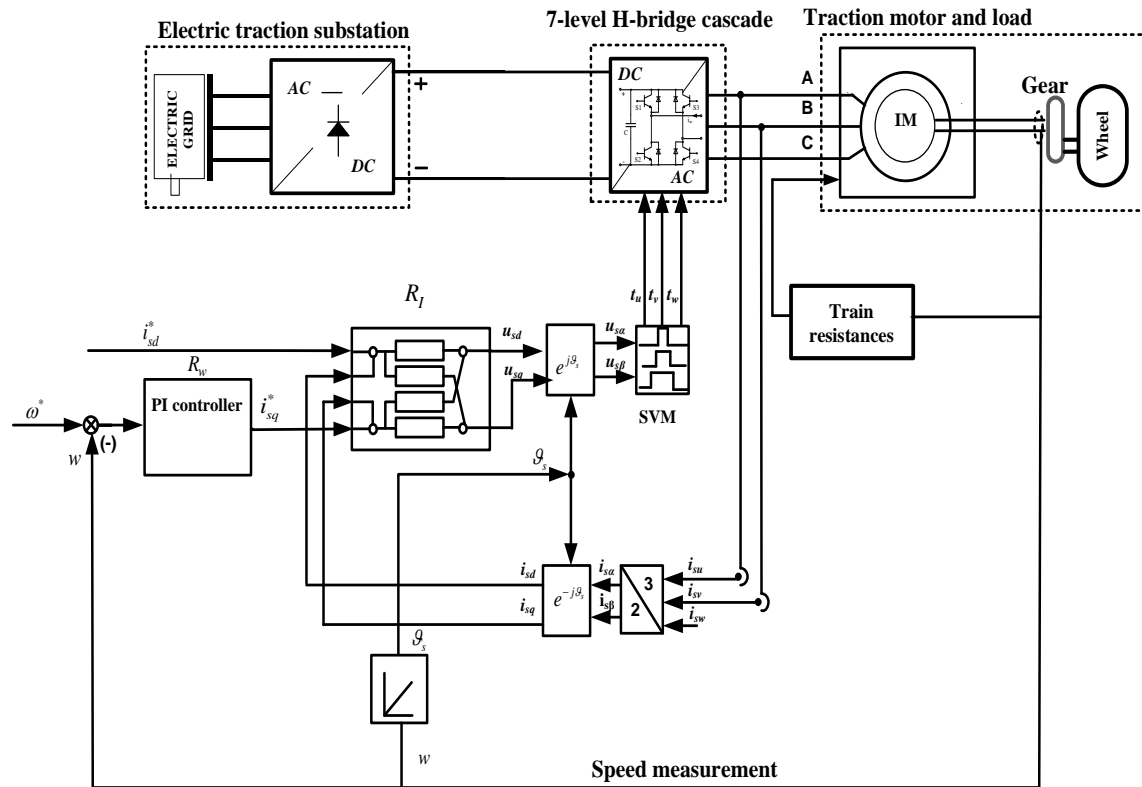


Figure 5. The structure of the cascaded H-bridge 7-level converter with the controllers for an IM used in an RTW

Table 2. Simulation with IM's parameters used railway traction motor

Parameters	Symbol	Value
DC voltage	U_{dc}	1000
Frequency of modulation	f_s	2000Hz
Power	P_{dm}	270 kW
Rated speed	n_{dm}	2880 rpm
Rated voltage	U_{dm}	400V
Pole pair	p	1
Power factor	$\cos \varphi$	0.9
Stator resistance	R_s	0.0138Ω
Rotor resistance	R_r	0.00773Ω
Rotor inductance	L_r	0.0078H
Mutual inductance	L_m	0.0077H
Voltage		750 VDC
Maximum speed for the train		80km/h

Case 1: simulation and evaluation of the 7-level inverters H-bridge cascaded

The typical working modes of multilevel inverters H-bridge cascaded from 3-level voltage to 7-level voltage through the following simulation scenario the linear modulation process with amplitude of the most significant voltage and activity diagrams as multilevel -level inverter as from 0 (s) - 0.3 (s). Simulation results 1-phase output phase voltage and the total harmonic distortion (THD) for multilevel inverter H-bridge are shown in Figures 6(a)-(f). According to the simulation results, Figure 6 found that the voltage waveform output phase inverter has enough voltage levels formats upon request. Output current is a sine wave and total harmonic distortion (THD) in the best 7-level inverse THD=9.72% compared with the three with THD=24.87% and five-level with THD=16.57%. Therefore, the 7-level inverse is suitable for feed to railway traction motor with low THD.

Case 2: simulation and evaluation of traction drive system using the cascaded H-bridge 7-level inverter

Some of the typical working RTM through the following simulation scenario as:

- From $t=1s$ to $t=3s$, the IM is operating at pull process with parameters:

$$\begin{aligned} t_{1s} &= 0(km/h) \\ t_{2s} &= 40(km/h) \\ t_{3s} &= 70(km/h) \end{aligned}$$

- From $t=3s$ to $t=6s$, the IM is operating at coasting process with parameters: $t_{6s} = 60(km/h)$.

c. From $t=6s$ to $t=8s$, the IM is operating at braking process with parameters:

$$t_{7s} = 5(km/h)$$

$$t_{8s} = 0(km/h)$$

Based on the simulation results of Figures 7(a)-(d) (in appendix), it is found that the current and speed controller has advantages. The actual speed matches the reference speed with a fast set time. However, the ripple torque is still high with $\Delta T_m\% = 30\%$. Therefore, this problem needs to be solved in the research to ensure low THD and low ripple torque. Moreover, it reduced the THD for the 7-level inverter H-bridge cascade with THD=9.72%.

Case 3: in the case of demonstrating the reliability of the railway traction drive system, the paper presented the case the rotor resistance increased by 50%.

Based on the simulation results of Figures 8(a)-(d) (in appendix), it found that the system was unstable, in which the speed dropped at the setting stage of the speed, and the ripple torque was large. Nevertheless, THD's 7-level inverter H-bridge value increased to 20.46%, and the format for output voltage is a sine.

5. CONCLUSION

The paper proposes a successful study of multi-level inverters in the railway traction drive system. An induction motor powers this the cascaded H-bridge 7-level inverter in railway traction, and this motor is controlled based on the FOC method. The simulation results have demonstrated that when the voltage level increases, the THD decreases, leading to an increase in the controller's efficiency. However, the design and calculation of this multi-level inverter are complicated when the number of voltage vectors increases rapidly with the number of voltage levels. In addition, this multi-level inverter has its advantages to create the desired speed response. However, in the case of sensitive motor parameters, this multi-level inverter still has a high THD, and railway traction drive system durability is not guaranteed. Hence, it is necessary to have a solution in the future, such as replacing the linear PI controller with nonlinear controllers or using the cascaded H-bridge 11-level inverter.

ACKNOWLEDGEMENTS

This project study was supported by all researchers and funding from the of School of Electrical and Electronics Engineering, Hanoi University of Science and Technology.

APPENDIX

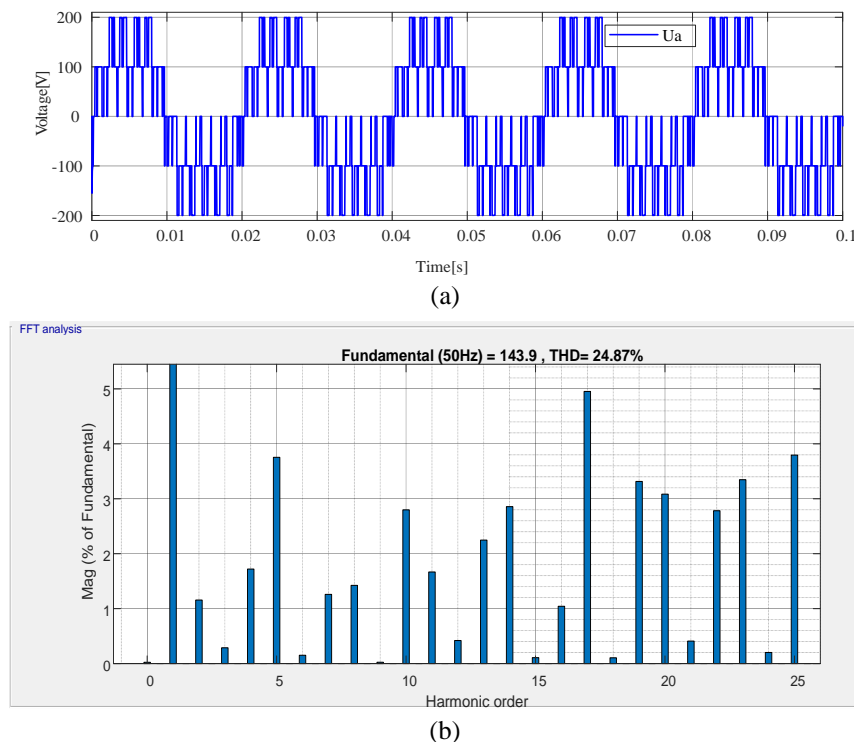


Figure 6. All response for; (a) the U_a phase voltage 3-level inverter H-bridge, (b) the THD of 3-level inverter H-bridge

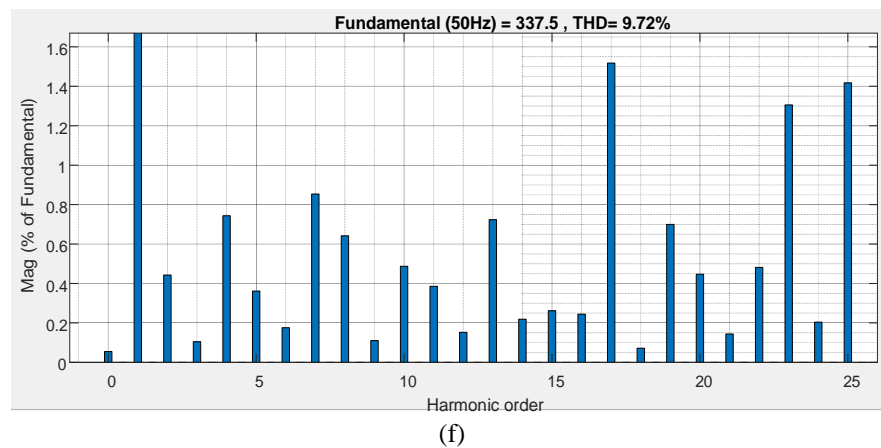
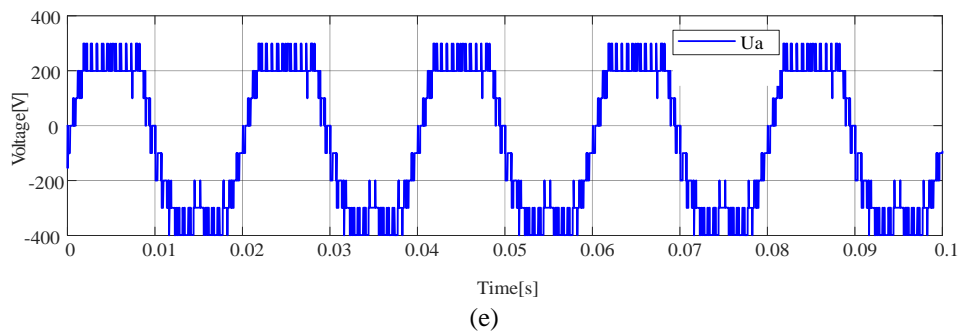
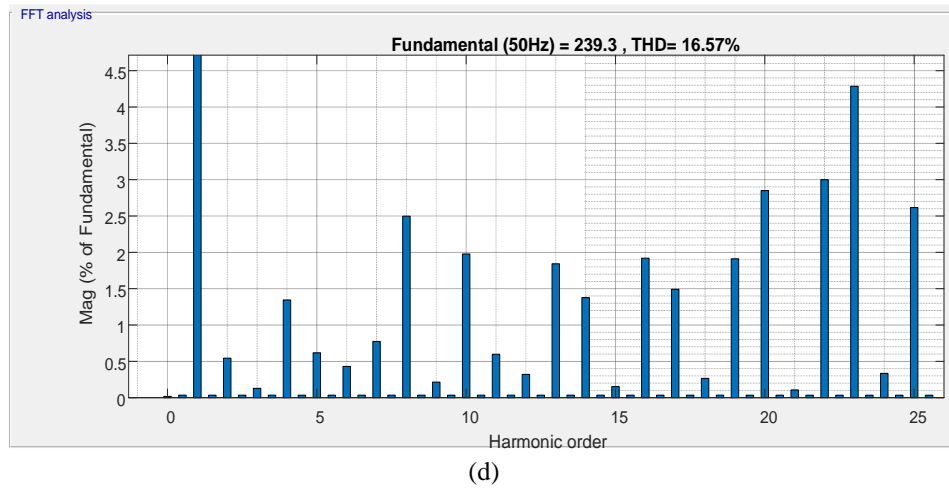
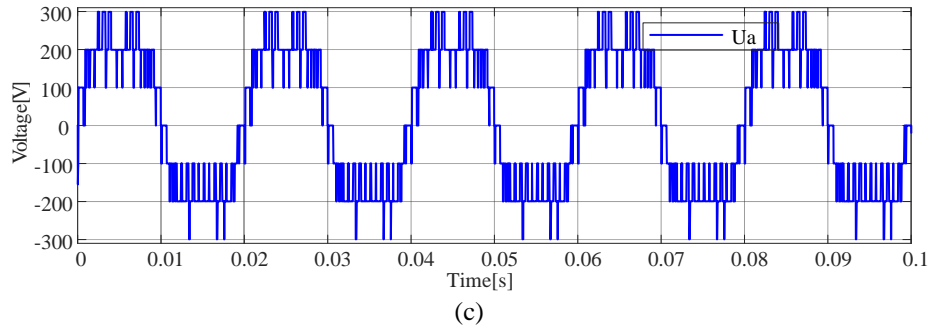


Figure 6. All response for; (c) the U_a phase voltage 5-level inverter H-bridge (d) the THD of 5-level inverter H-bridge, (e) the U_a phase voltage 7-level inverter H-bridge, and (f) the THD of 7-level inverter H-bridge (continue)

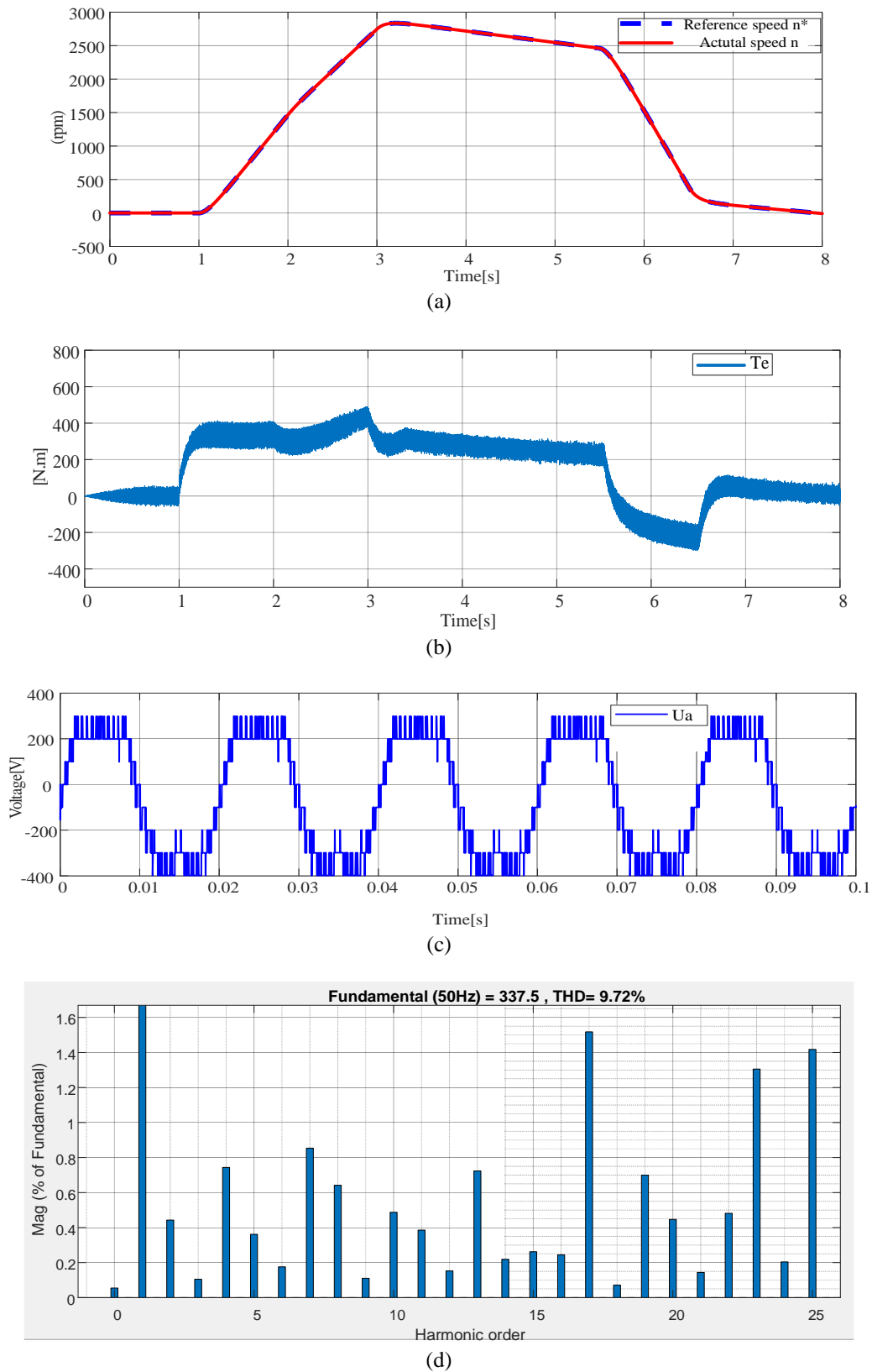


Figure 7. All simulation results in the case is R_r is constant for; (a) speed responses, (b) the torque response, (c) the U_a phase voltage and (d) the total harmonic distortion

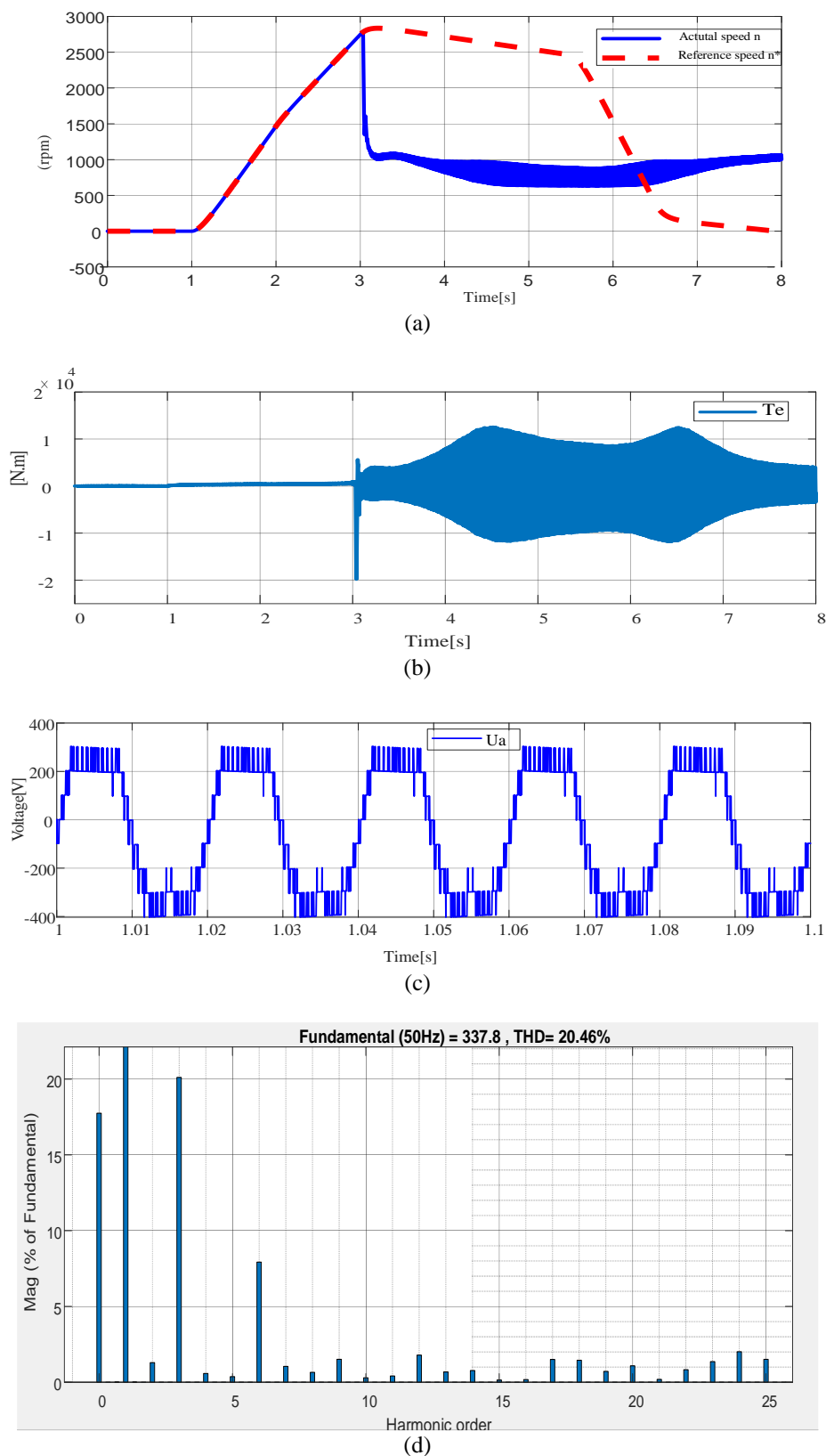





Figure 8. All simulation results in the case is R_r is increasing to 50% for; (a) speed responses, (b) the torque response, (c) the U_a phase voltage and (d) the total harmonic distortion




REFERENCES

- [1] L. Frederick and G. K. Dubey, "AC motor traction drives — A status review," *Sadhana*, vol. 22, p. 855, 1997, doi: 10.1007/BF02745849.
- [2] M. Nicolae and I. Bojoi, "A control strategy for an induction motor used for vehicular traction and/or positioning systems with variable speeds," *2012 International Conference on Applied and Theoretical Electricity (ICATE)*, 2012, pp. 1-6, doi: 10.1109/ICATE.2012.6403425.
- [3] A. F. Abouzeid *et al.*, "Control Strategies for Induction Motors in Railway Traction Applications," *Energies*, vol. 13, no. 3, p. 700, 2020, doi: 10.3390/en13030700.
- [4] N. P. Quang and J. -A. Dittrich, "Vector control of three-phase AC machines - System development in the practice," 2nd edition, Berlin Heidelberg: Springer-Verlag.
- [5] R. J. Hill, "Electric railway traction. Part 3. Traction power supplies," *Power Engineering Journal*, vol. 8, no. 6, pp. 275-286, Dec. 1994, doi: 10.1049/pe:19940604.
- [6] S. K. Bade and V. A. Kulkarni, "Analysis of Railway Traction Power System Using Renewable Energy: A Review," *2018 International Conference on Computation of Power, Energy, Information and Communication (ICCPEIC)*, 2018, pp. 404-408, doi: 10.1109/ICCPEIC.2018.8525206.
- [7] S. Nategh, D. Lindberg, R. Brammer, A. Boglietti, and O. Aglen, "Review and Trends in Traction Motor Design: Electromagnetic and Cooling System Layouts," *2018 XIII International Conference on Electrical Machines (ICEM)*, 2018, pp. 2600-2606, doi: 10.1109/ICELMACH.2018.8506817.
- [8] A. Steimel, *Electrical Traction-Motive Power and Energy Supply - Basics and Practical Experience*, Munich: Oldenbourg Industrieverlag, 2008.
- [9] A. Steimel, *Electric Traction - Motive Power and Energy Supply, Basics and Practical Experience*, 2nd edition, Virginia: Stylus Pub Llc., 2014.
- [10] C. M. Van, T. N. Xuan, P. V. Hoang, M. T. Trong, S. P. Cong, and L. N. Van, "A Generalized Space Vector Modulation for Cascaded H-bridge Multi-level Inverter," *2019 International Conference on System Science and Engineering (ICSSE)*, 2019, pp. 18-24, doi: 10.1109/ICSSE.2019.8823465.
- [11] G. I. Orfanoudakis, S. M. Sharkh, M. A. Yuratich, and M. A. Abusara, "Loss comparison of two and three-level inverter topologies," *5th IET International Conference on Power Electronics, Machines and Drives (PEMD 2010)*, 2010, pp. 1-6, doi: 10.1049/cp.2010.0172.
- [12] S. Pradhan, "Multilevel Inverter Based Electric Traction Drives," M.S. Thesis, Department of Electrical Engineering, National Institute of Technology, Rourkela, 2012.
- [13] B. Wu and M. Narimani, "Diode-Clamped Multilevel Inverters," in *High-Power Converters and AC Drives*, 2nd Edition, Hoboken, New Jersey: Wiley, 2016.
- [14] S. Shi, X. Wang, S. Zheng, and F. Xia, "A new diode-clamped multilevel inverter for capacitor voltage balancing," *Progress In Electromagnetics Research M*, vol. 52, pp. 181-190, 2016, doi: 10.2528/PIERM16100603.
- [15] L. G. Franquelo, J. Rodriguez, J. I. Leon, S. Kouro, R. Portillo, and M. A. M. Prats, "The age of multilevel converters arrives," *IEEE Industrial Electronics Magazine*, vol. 2, no. 2, pp. 28-39, June 2008, doi: 10.1109/MIE.2008.923519.
- [16] M. Es-Saadi, M. Khafallah, and H. Chaikhy, "Using the Five-Level NPC Inverter to Improve the FOC Control of the Asynchronous Machine," *International Journal of Power Electronics and Drive System*, vol. 9, no. 4, pp. 1457-1466, 2018, doi: 10.11591/ijpeds.v9.i4.pp1457-1466.
- [17] A. S. R. A. Subki *et al.*, "Analysis on three phase cascaded H-bridge multilevel inverter based on sinusoidal and third harmonic injected pulse width modulation via level shifted and phase shifted modulation technique," *International Journal of Power Electronics and Drive Systems*, vol. 12, no. 1, pp. 160-169, 2021, doi: 10.11591/ijpeds.v12.i1.pp160-169.
- [18] F. Z. Peng and Jih-Sheng Lai, "Dynamic performance and control of a static VAR generator using cascade multilevel inverters," *IEEE Transactions on Industry Applications*, vol. 33, no. 3, pp. 748-755, 1997, doi: 10.1109/28.585865.
- [19] V. T. Ha, P. T. Giang, and V. H. Phuong, "T-Type Multi-Inverter Application for Traction Motor Control," *Engineering, Technology & Applied Science Research*, vol. 12, no. 2, pp. 8321-8327, 2022, doi: 10.48084/etasr.4776.
- [20] J. Rodriguez, S. Bernet, B. Wu, J. O. Pontt, and S. Kouro, "Multilevel Voltage-Source-Converter Topologies for Industrial Medium-Voltage Drives," *IEEE Transactions on Industrial Electronics*, vol. 54, no. 6, pp. 2930-2945, Dec. 2007, doi: 10.1109/TIE.2007.907044.
- [21] H. Gupta, A. Yadav, and S. Maurya, "Dynamic performance of cascade multilevel inverter based STATCOM," *2016 IEEE 1st International Conference on Power Electronics, Intelligent Control and Energy Systems (ICPEICES)*, 2016, pp. 1-4, doi: 10.1109/ICPEICES.2016.7853479.
- [22] P. Cortés, A. Wilson, S. Kouro, J. Rodriguez, and H. Abu-Rub, "Model Predictive Control of Multilevel Cascaded H-Bridge Inverters," in *IEEE Transactions on Industrial Electronics*, vol. 57, no. 8, pp. 2691-2699, Aug. 2010, doi: 10.1109/TIE.2010.2041733.
- [23] A. H. Ali, H. S. Hamad, and A. A. Abdulrazzaq, "An adaptable different-levels cascaded h-bridge inverter analysis for PV grid-connected systems," *International Journal of Power Electronics and Drive System*, vol. 10, no. 2, pp. 831-841, 2019, doi: 10.11591/ijpeds.v10.i2.pp831-841.
- [24] S. N. Rao, D. V. A. Kumar, and C. S. Babu, "Implementation of Cascaded based Reversing Voltage Multilevel Inverter using Multi Carrier Modulation Strategies," *International Journal of Power Electronics and Drive Systems*, vol. 9, no. 1, pp. 220-230, 2018, doi: 10.11591/ijpeds.v9.i1.pp220-230.
- [25] E. Shravan and R. A. Murugan, "Survey on Multilevel Inverter with Less Number of Switches for Different Loads," *SSRG International Journal of Electrical and Electronics Engineering*, vol. 5, no. 6, pp. 16, 25, 2018, doi: 10.14445/23488379/IJEEE-V5I6P104.




BIOGRAPHIES OF AUTHORS

Vo Thanh Ha    received the B.S degree in Control, and Automation Engineering from Thai Nguyen University of Technology, Vietnam, in 2002. She received the Master's degree from Hanoi University of Science and Technology, Vietnam, in 2004. She received a Ph.D. degree from Hanoi University of Science and Technology, Vietnam, in 2020, both in Control and Automation Engineering. She has worked at the University of Transport and Communications as a lecturer since 2005. Her current areas: electrical drive system and electric vehicle. She can be contacted at email: vothanhha.ktd@utc.edu.vn.



Phuong Vu    received his B.S., M.S., and Ph.D. degrees from Hanoi University of Science and Technology, Vietnam, in 2006, 2008, and 2014, respectively, all in Control Engineering and Automation. Since 2006 he has been employed at Hanoi University of Science and Technology, where he is a lecturer and researcher at school of electrical engineering. His research interests include modeling and controlling of power electronics converters for applications such as photovoltaic, wind system, electrical machine drive. He can be contacted at email: phuong.vuhoang@hust.edu.vn.



Pham Thi Giang    was born in 1997 and is a master's student in the 2020-2022 course in automation at Hanoi University of Science and Technology (HUST). Currently, he is a lecturer specializing in automation at the University of Economics and Industry. The main research direction is electric drive control and power electronics. She can be contacted at email: phamthigiang261097@gmail.com.